Rhodium-catalyzed reductive modification of pyrimidine nucleosides, nucleotide phosphates, and sugar nucleotides

Neil P.J. Price, Michael A. Jackson, Karl E. Vermillion, Judith A. Blackburn, Trina M. Hartman

PII: S0008-6215(19)30413-6

DOI: https://doi.org/10.1016/j.carres.2019.107893

Reference: CAR 107893

To appear in: *Carbohydrate Research*

Received Date: 12 July 2019

Revised Date: 26 November 2019

Accepted Date: 13 December 2019

Please cite this article as: N.P.J. Price, M.A. Jackson, K.E. Vermillion, J.A. Blackburn, T.M. Hartman, Rhodium-catalyzed reductive modification of pyrimidine nucleosides, nucleotide phosphates, and sugar nucleotides, *Carbohydrate Research* (2020), doi: https://doi.org/10.1016/j.carres.2019.107893.

GRAPHICAL ABSTRACT

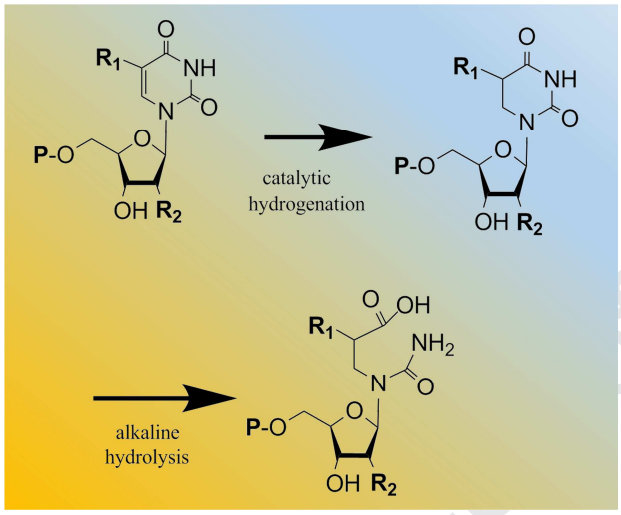

HIGHLIGHTS

- Quantitative catalytic hydrogenation of pyrimidines.
- Nucleosides, nucleotide phosphates, and sugar nucleotides.
- Ring opening of 5,6-DH-uridyl and 5,6-DH-thymidyl bases.

Rhodium-catalyzed reductive modification of pyrimidine nucleosides, nucleotide phosphates, and sugar nucleotides.

Neil P. J. Price*, Michael A. Jackson, Karl E. Vermillion, Judith A. Blackburn, Trina M. Hartman

Agricultural Research Service, U.S. Department of Agriculture, National Center for Agricultural Utilization Research, Peoria, IL, U.S.A.

*Correspondence: Dr. N. P. J. Price, Agricultural Research Service, U. S. Department of Agriculture, USDA-ARS, National Center for Agricultural Utilization Research, 1815 N University Street, Peoria, IL, 61604, U.S.A.

E-mail: neil.price@ars.usda.gov

ABSTRACT

Nucleosides and nucleotides are a group of small molecule effectors and substrates which include sugar nucleotides, purine and pyrimidine-based nucleotide phosphates, and diverse nucleotide antibiotics. We previously reported that hydrogenation of the nucleotide antibiotic tunicamycin leads to products with reduced toxicity on eukaryotic cells. We now report the hydrogenation of diverse sugar nucleosides, nucleotide phosphates, and pyrimidine nucleotides. UDP-sugars and other uridyl and thymidinyl nucleosides are quantitatively reduced to the corresponding 5,6-dihydro-nucleosides. Cytidyl pyrimidines are reduced, but the major products are the corresponding 5,6-dihydrouridyl nucleosides resulting from a deamination of the cytosine ring.

Keywords: 5,6-dihydropyrimidines, catalytic hydrogenation, pyrimidines, sugar nucleotides.

1. Introduction

Nucleoside antibiotics are a diverse group of small metabolites that include antibacterial, antiviral, and antifungal agents [1–3]. Many of these are either antibacterial (e.g., caprazamycin, capuramycin, liposidomycin, tunicamycin, muraymycin, and mureidomycin), or antifungal (e.g., polyoxins and nikkomycins) [4–7]. Other nucleosides and nucleotides are small molecule effectors and substrates such as sugar nucleotides, uridine monophosphate (UMP), adenosine monophosphate (AMP), cyclic AMP, *S*-adenosylmethionine (SAM), and purines involved in sulfur metabolism (adenosine phosphosulfates, APS, and (P)APS). The binding, and hence the activity, of several of these inhibitors and substrates is at least partially determined by interactions between the target protein and the nucleotide base motif, often via a planar, pseudo-aromatic π-π stacking complex [8]. Hydrogenation of the carbon-5 – carbon-6 double bond in the uridyl motif of tunicamycin, for example, leads to a modified, non-planar 5,6-dihydrouridyl substituent, and with a concomitant loss of biological activity and toxicity on eukaryotic cells [9, 10]. The rhodium-catalyzed hydrogenation of the uridyl base is of interest because the product 5,6-dihydrouridyl base is non-aromatic and assumes a non-planar chair configuration [8, 9]. This is also seen for the streptovirudins, a group of tunicamycin structural variants that have a naturally-occurring 5,6-dihydrouracil group replacing the more common uracil moiety [11, 12].

In the current paper, we have investigated the breadth of this catalytic reduction as applied to three pyrimidine nucleosides (uridine, thymidine, and cytidine), four nucleotide phosphates (UMP, UDP, UTP, and CMP), and four sugar nucleotides (UDP-Glc, UDP-Gal, UDP-GlcNAc, and UDP-glucuronic acid). Similar approaches have been investigated previously [13–16]. Especially of interest is the applicability of the hydrogenation to diverse nucleoside bases, the effect of the multiple phosphate groups, and the overall stability, especially with

respect to the generally labile sugar nucleotides. Moreover, this work provides access to a group of reduced nucleotides suitable for biological testing as potential antibacterial or antifungal agents.

2. Results and Discussion

2.1. Catalytic hydrogenation of sugar nucleotides. Sugar nucleotides may differ in both the nucleotide and monosaccharide motifs and are notoriously susceptible to hydrolysis during handling. Under the conditions described in the Experimental section 3.2., various sugar nucleotides were hydrogenated as exemplified by UDP-*N*-acetylglucosamine (UDP-GlcNAc, Fig. 1). NMR analysis of the 5,6-dihydro-UDP-GlcNAc (5,6-DHU-GlcNAc) showed two carbohydrate anomeric signals are apparent for the β-ribosyl H-1′ (5.84 ppm, 87.3 ppm) and the α-*N*-acetylglucosaminyl H-1′ (5.44 ppm, 94.8 ppm). The completeness of the reaction is evident from the absence of uridyl alkene signals (Fig. 1.A). The product 5,6-DHU-GlcNAc was also apparent from the 2 Da mass increase in the MALDI/MS spectra ($[M+H]^+$ = *m/z* 654.5; $[M+Na]^+$ = *m/z* 676.5) (Fig. 1.B and C) due to hydrogenation of the uridyl 5,6-double bond. The analogous uridine MALDI/MS ions were observed at *m/z* 652.5 and *m/z* 674.4, respectively (Fig. 1.B).

Catalytic hydrogenation of three other uridyl sugar nucleotides was also undertaken. HSQC NMR analysis showed that the UDP-Glc, UDP-Gal and UDP-GlcA are cleanly reduced to 5,6-dihydro-UDP-Glc, 5,6-dihydro-UDP-Gal and 5,6-dihydro-UDP-GlcA, respectively (Fig. 2, supplementary Table 1). The β-ribosyl H-1′ anomeric protons were observed at 5.85, 5.85 and

5.84 ppm, respectively, with corresponding ^{13}C-NMR chemical shifts at 86.7, 86.9, and 86.9 ppm. The α-anomer NMR signals for the corresponding hexose sugars were apparent at 5.52/94.6, 5.50/94.8, and 5.52/94.8 ppm, respectively. The hydrogenated C5 and C6 positions in the base moieties were apparent at 30.2 and 36.0 ppm, respective, with corresponding H5 and H6-a,b ^{1}H-NMR signals at 2.73 ppm (overlapped) and 3.51, 3.61 ppm (Fig. 2). That the hydrogenations had proceeded to completion is evident from the complete disappearance of H5 and H6 alkene proton signals (7.9 and 5.9 ppm, respectively) or the corresponding C5 and C6 ^{13}C-NMR signals at 142 and 102 ppm.

2.2. Hydrogenation of nucleotide phosphates. The effect of phosphate groups on the hydrogenation reaction was investigated next, as exemplified by the reduction of UMP, UDP, and UTP (Fig. 3). MALDI/MS analysis showed the expected 2 Da mass increase due to reduction of the uridyl 5,6-double bonds. Hence, the $[M+H]^+$, *m/z* 347.3 and $[M+Na]^+$, *m/z* 369.3 ions are increased by 2 Da to *m/z* 349.3 and 371.3, respectively, for 5,6-DH-UMP. Similarly, *m/z* 427.2, 449.2, 471.2, and 493.1 are increase by 2 Da to *m/z* 429.2, 451.2, 473.2, and 495.1 for 5,6-DH-UDP; and *m/z* 507.3, 529.2, 551.3, and 573.2 increase by 2 Da to *m/z* 509.3, 531.3, 553.3, and 575.3 for 5,6-DH-UTP. NMR analysis shows an absence of 5,6-alkene signals, confirming the complete reduction of these products. Each has a single ribosyl-1' anomeric signal in the HSQC spectra at 5.82 ppm, 86.5 – 87.1 ppm, and the uridyl 5 and 6 a,b signals are also apparent at 2.72 ppm, 29.9 – 30.6 ppm and 3.52 – 3.61 ppm, 35.8 ppm, respectively (Fig. 2, supplementary Table 1).

2.3. Catalytic hydrogenation of other pyrimidine nucleosides. The most common pyrimidine nucleosides, uridine, cytidine, and thymidine, differ structurally in the base substituent and the pentose sugar motif. Under the catalytic conditions described uridine is quantitatively hydrogenated to 5,6-dihydrouridine (5,6-DHU), as shown by both MALDI/MS and NMR analysis (supplementary Fig. S.1). The MS molecular ions for uridine ($[M+H]^+$ = *m/z* 245.2, $[M+Na]^+$ = *m/z* 267.2) are converted to 5,6-DHU ($[M+H]^+$ = *m/z* 247.3, $[M+Na]^+$ = *m/z* 269.3), with the mass increase of 2 Da resulting from reduction of the uridyl double bond. NMR analysis also showed that the reaction is quantitative, the resulting 5,6-DHU lacking any residual NMR signals in the alkene region typical of uridine. A single ribosyl-1' anomeric signal is apparent at 5.80 ppm/87 ppm, and the reduced uridyl H5 and H6 signals at 3.7 and 3.5 ppm, respectively (supplementary Fig. S.1.). Thymidine is similarly converted to 5,6-dihydrothymidine (5,6-DHT), with an analogous mass increase of 2 Da, with the characteristic anomeric ribosyl-1' signals at 6.25 ppm and 82 ppm, respectively (supplementary Fig. S.1, supplemental Table 1). Hence, the hydrogenation is unaffected by the 5-methyl substituent on the thymine ring, and both thymidine and uridine are quantitively reduced to the corresponding 5,6-anhydronucleosides. Note that the 5,6-DHT is assumed to contain a new chiral carbon-6, although this has not been confirmed by the current methods.

2.4. Cytidine nucleosides. It was noted that the hydrogenation of the cytidine-based nucleoside and nucleotides (cytidine, CMP, CDP, and CTP) did not proceed as for the respective uridyl or thymidyl analogs. Catalytic reduction of cytidine, for example, resulted in an almost complete de-amination of the cytidyl ring, with the major product characterized by ^{1}H-NMR and MALDI/MS as 5,6-dihydrouridine (Fig. 4). The anticipated product, 5,6-dihydrocytidine, was

only produced at about 10% yield during this reaction (Fig. 4). In analogous reactions with CMP, CDP, and CTP de-amination also occurred, and the major products obtained were the analogous 5,6-dihydrouridyl phosphate nucleotides (data not shown). The deamination of cytidine and cytosine at acidic pH is well known [17, 18], and indeed also occurs enzymatically by cytidine deaminase during pyrimidine salvaging [19]. However, the observed de-amination of the cytidine nucleotides during catalytic hydrogenation was unexpected, and this therefore precludes the production of 5,6-dihydrocytidine nucleosides by this route.

2.5. Base-catalyzed hydrolytic ring opening.

Base-catalyzed hydrolytic ring opening of the 5,6-dihydrouridyl ring of hydrogenated tunicamycins, and some other nucleotides, is known [9, 10], but not for other pyrimidine nucleosides, nucleotide phosphates, or nucleotide sugars. Hence, the hydrogenation products obtained from above were hydrolyzed with aqueous sodium hydroxide under conditions described previously [10]. The products were analyzed by MALDI/MS, ^{1}H-NMR, ^{13}C-NMR and HSQC-NMR (supplementary Table 1, supplementary Fig. S.2). Under these mild conditions (0.25 M aqueous sodium hydroxide for 18 h at ambient temperature) the uridyl and thymidyl nucleosides were quantitatively hydrolyzed, resulting in opening of the base ring without cleavage of the ribosyl or 2-deoxyribosyl *N*-glycosidic bonds (Scheme 1). This was evident from MALDI/MS due to the 18 Da mass increase which occurs during the hydrolysis of the amide bond in the reduced nucleotide base ring, and from the NMR analysis of the nucleoside 1′, 5, and 6 protons (supplementary Fig. S.2., supplementary Table 1). Noticeably, the often labile sugar nucleotides were hydrolytically base opened but the rest of the molecule was unaffected, with no hydrolysis of the glycosidic or phosphate bonds (e.g. 5,6-DHU-GlcNAc, supplementary

Fig. S.2.C). The corresponding non-hydrogenated nucleosides were resistant to base hydrolyzed, and were completely stable under these alkaline conditions (data not shown).

3. Experimental Section

3.1. Materials and Instrumentation

All chemicals and solvents, except for the catalyst (5 wt% Rh/Al_2O_3 from BASF Engelhard, Iselin, NJ) were obtained from Sigma-Aldrich Inc., St Louis, MO, USA. NMR spectra were run in D_2O at 27 ºC using a Bruker Avance III instrument (Bruker BioSpin, Billerica, MA, USA). MALDI-TOF mass spectra were recorded using a Bruker-Daltonics Microflex instrument (Bruker-Daltonics, Billerica, MA, USA) in reflectron mode. The matrix used was 2,5-dihydrobenzoic acid.

3.2. Hydrogenation conditions

The hydrogenations were undertaken as described previously [10]. Briefly, the nucleoside starting material (30 mg) in aqueous solution (3 mL) were reacted for 3 hours at room temperature (21 ° C). Catalyst (5 wt% Rh/Al_2O_3; 20 mg) was introduced at the start of the reactions, and hydrogen gas was bubbled through at atmospheric pressure. The products were recovered by filtration to remove the catalyst, followed by lyophilization to remove the water. MALDI/MS spectra were recorded on the aqueous solutions immediately after removal of the catalyst. The lyophilized product residues were re-dissolved in deuterated water for analysis by NMR (^{1}H-NMR, ^{13}C-NMR, HSQC) without further purification. For the base-catalyzed ring opening reactions, the hydrogenated nucleosides were treated at room temperature for 18 h using

aqueous sodium hydroxide (0.25 M). After neutralization with HCl (0.25M) the samples were analyzed by NMR and MALDI/MS.

Acknowledgements

The authors thank C. D. Skory (ARS-USDA, Peoria, IL, USA) for the initially review of the manuscript. Mention of any trade names or commercial products is solely for the purpose of providing specific information and does not imply recommendation or endorsement by the US Department of Agriculture. USDA is an equal opportunity provider and employer.

References

1. M. Serpi, V. Ferrari, F. Pertusati J. Med. Chem., 59 (2017), pp. 10343−10382

2. G. Niu, H. Tan Trends Microbiol., 23 (2015), pp. 110−119

3. W. Chen, J. Qi, P. Wu, D. Wan, J. Liu, X. Feng, Z. Deng Z J. Ind. Microbiol. Biotechnol., 43 (2016), pp. 401−417

4. W. Winn, R. J. M. Goss, K. Kimura, T. D. H. Bugg Nat. Prod. Rep., 27 (2010), pp. 279−304

5. S. Rachakonda, L. Cartee Curr. Med. Chem., 11 (2004), pp. 775−793

6. K. Kimura, T. D. H. Bugg Nat. Prod. Rep., 20 (2003), pp. 252−273

7. K. Isono Pharmacol. Ther., 52 (1991), pp. 269−286

8. K. M. Ivanetich, D. V. Santi Prog. Nucleic Acid Res. Mol. Biol., 42 (1992), pp. 127−156

9. N. P. Price, T. M. Hartman, J. Li, K. K. Velpula, T. A. Naumann, M. R. Guda, B. Yu, K. M. Bischoff J. Antibiot., 70 (2017), pp. 1070−1077

10. N. P. Price, M. A. Jackson, K. E. Vermillion, J. A. Blackburn, J. Li, B. Yu J. Antibiot., 70 (2017), pp. 1122−1128

11. K. Eckardt, W. Ihn, D. Tresselt, D. Krebs J. Antibiot., 34 (1981), pp. 1631−1632

12. K. Eckardt, H. Thrum, G. Bradler, E. Tonew, M. Tonew J Antibiot., 28 (1975), pp. 274−279

13. W. E. Cohn, D. G. Doherty J. Am. Chem. Soc., 78 (1956), pp. 2863–2866

14. N. K. Kochetkov, E, I. Budovskii, V. N. Shibaev, G. I Eliseeva Russ. Chem. Bull. 14 (1965), pp. 884–885

15. P. Cerutti, K. Ikeda, B. Witkop J. Am. Chem. Soc. 87 (1965), pp 2505–2507

16. P. Cerutti, Y. Kondo, W. R. Landis, B. Witkop J. Am. Chem. Soc. 90(1968), pp. 771–775

17. R. Shapiro, R. S. Klein Biochemistry, 5 (1966), pp. 2358–2362

18. V. Labet, C. Morell, T. Douki, J. Cadet, L. A. Eriksson, A. Grand J. Phys. Chem., 114 (2010), pp. 1826-1834

19. S. Vincenzetti, G. De Sanctis, S. Costanzi, G. Cristalli, P. Mariani, G. Mei, J. Neuhard, P. Natalini, V. Polzonetti, A. Vita Protein Eng., 16 (2004), pp. 1055–1061

List of Table, Figures, and Schemes

Figure 1. HSQC-NMR spectrum of 5,6-dihydro-UDP-*N*-acetylglucosamine (A), and MALDI/MS spectra of UDP-*N*-acetylglucosamine before (B) and after hydrogenation (C). The molecular adduct ions $[M+H]^+$, *m/z* 652 and $[M+Na]^+$, *m/z* 674 are increase by 2 mass units due to quantitative hydrogenation of the 5,6-uridyl double bond.

Figure 2. ^{1}H-NMR, ^{13}C-NMR, and HSQC spectra of other hydrogenated sugar nucleotides. (A) 5,6-DHU-Glc; (B) 5,6-DHU-Gal; and (C) 5,6-DHU-glucuronic acid.

Figure 3. Effects of phosphate groups. HSQC-NMR spectra of (A) 5,6-dihydrouridine monophosphate; (B) 5,6-dihydrouridine diphosphate; and (C) 5,6-dihydrouridine triphosphate. Corresponding MALDI/MS spectra before (D, E, F) or after (G, H, I) hydrogenation. Molecular adduct ions ($[M+H]^+$ and $[M+Na]_n^+$) are increase by 2 Da after hydrogenation.

Figure 4. De-amination of 5,6-dihydrocytidine nucleosides during hydrogenation. ^{1}H-NMR spectra of (A). 5,6-dihydrouridine from hydrogenation of uridine; (B). hydrogenated cytidine. Both samples are predominantly converted to 5,6-dihydrouridine. The anticipated 5,6-dihydrocytidine is shown as a minor product indicated by the black arrows.

Scheme 1. Catalytic hydrogenation and alkaline-catalyzed ring opening of pyrimidine sugar nucleosides, nucleotide phosphates, and nucleosides.

Supplementary Table 1. NMR Chemical Shifts for the Characteristic Ribosyl-1′ and Nucleotide Base-5,6 Positions.

Supplementary Figure S.1. Catalytic hydrogenation products 5,6-dihydrouridine (top) and 5,6-dihydrothymidine (lower). Shown are HSQC-NMR spectra (A, B), and MALDI/MS spectra either before (C, D) or after (E, F) hydrogenation. Molecular ions ($[M + H]^+$ and $[M + Na]^+$) are increased by 2 Da after hydrogenation due to reduction of the 5,6-double bond in the base.

Supplementary Figure S.2. HSQC-NMR spectra of the alkaline hydrolyzed ring-opened pyrimidine nucleotides. (A) 5,6-dihydrouridine diphosphate; (B) 5,6-dihydro-thymidine; and (C) 5,6-dihydrouridine-UDP-N-acetylglucosamine.

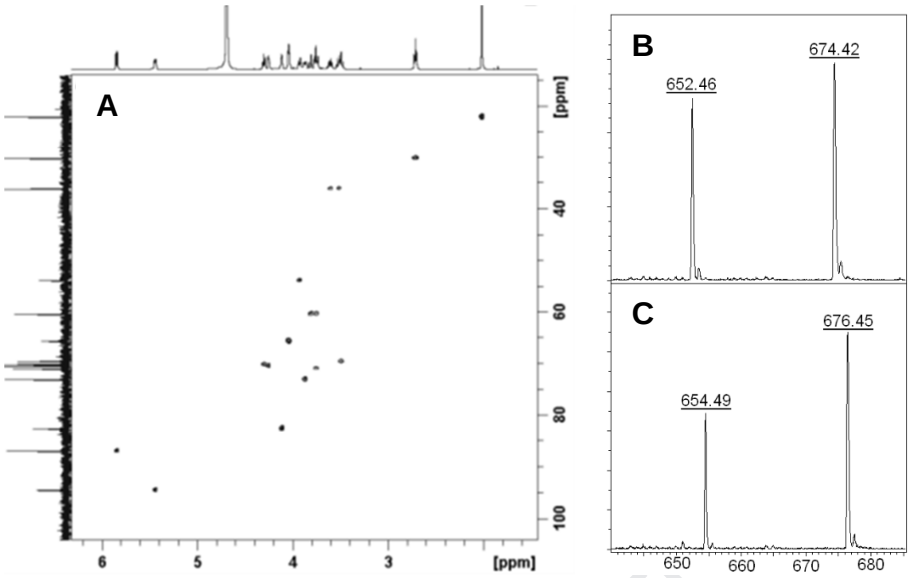

Figure 1. HSQC-NMR spectrum of 5,6-dihydro-UDP-*N*-acetylglucosamine (A), and MALDI/MS spectra of UDP-*N*-acetylglucosamine before (B) and after hydrogenation (C). The molecular adduct ions $[M+H]^+$, *m/z* 652 and $[M+Na]^+$, *m/z* 674 are increase by 2 mass units due to quantitative hydrogenation of the 5,6-uridyl double bond.

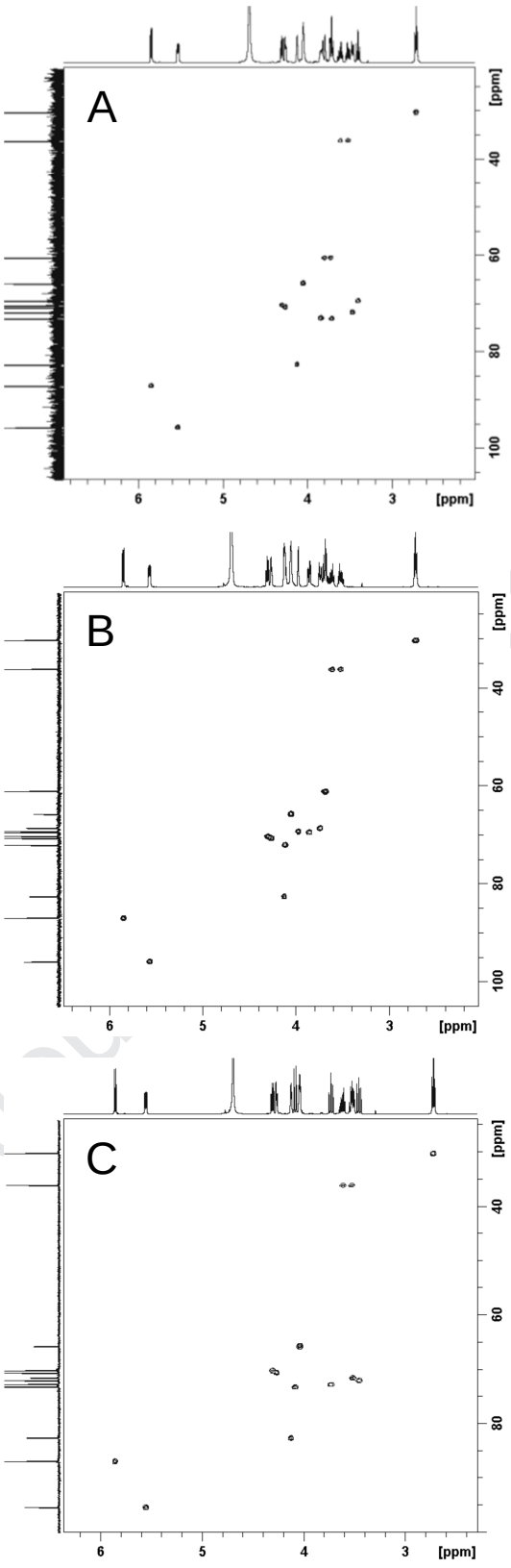

Figure 2. ^{1}H-NMR, ^{13}C-NMR, and HSQC spectra of other hydrogenated sugar nucleotides. (A) 5,6-DHU-Glc; (B) 5,6-DHU-Gal; and (C) 5,6-DHU-glucuronic acid.

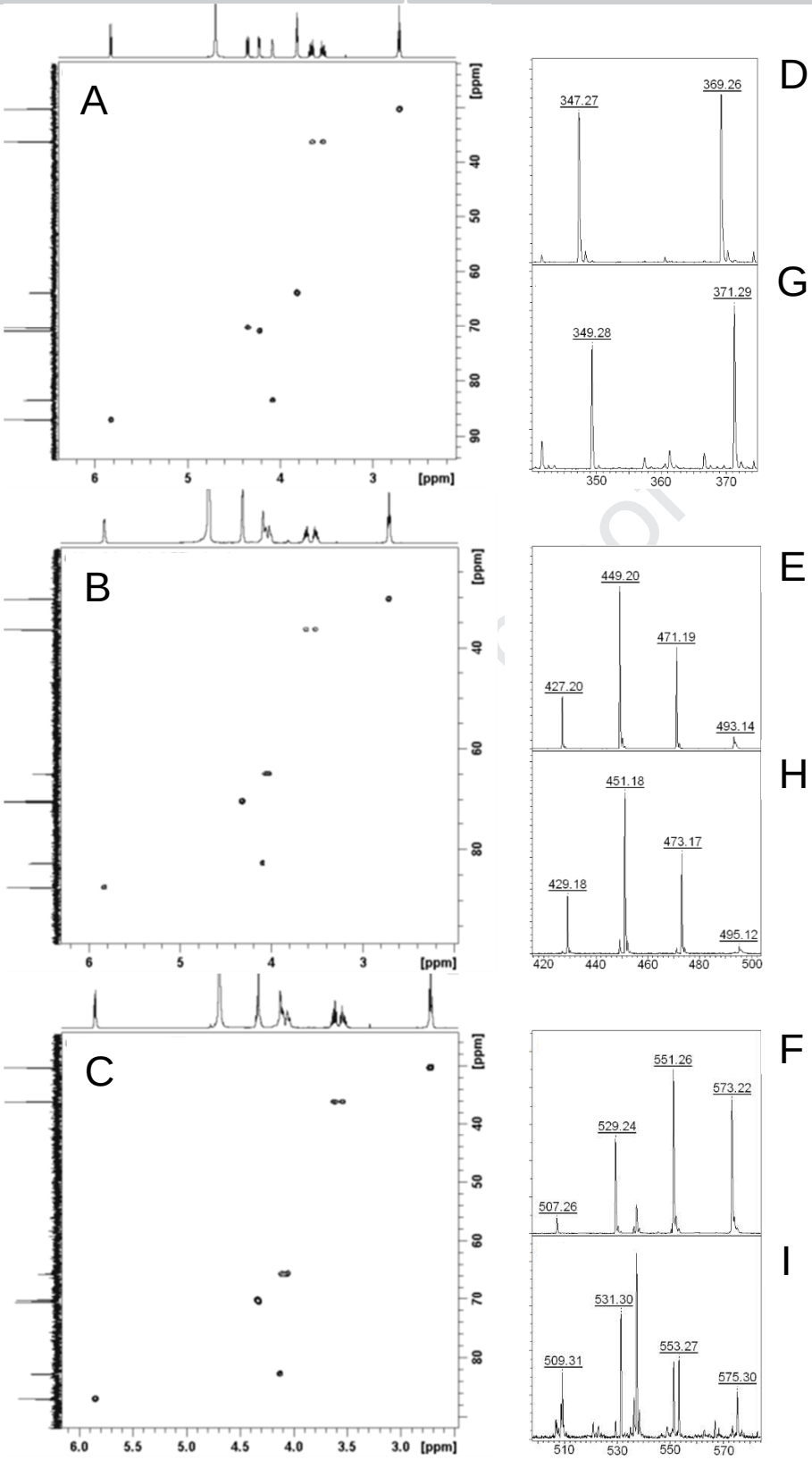

Figure 3. Effects of phosphate groups. HSQC-NMR spectra of (A) 5,6-dihydrouridine monophosphate; (B) 5,6-dihydrouridine diphosphate; and (C) 5,6-dihydrouridine triphosphate. Corresponding MALDI/MS spectra before (D, E, F) or after (G, H, I) hydrogenation. Molecular adduct ions ($[M+H]^+$ and $[M+Na]_n^+$) are increase by 2 Da after hydrogenation.

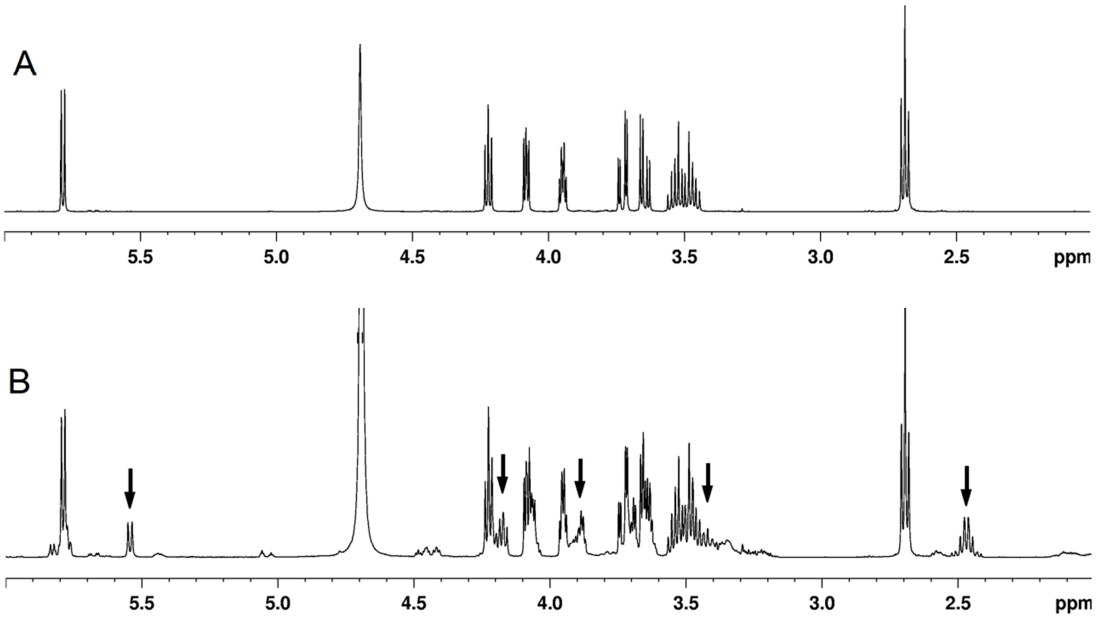

Figure 4. De-amination of 5,6-dihydrocytidine nucleosides during hydrogenation. ^{1}H-NMR spectra of (A) hydrogenated uridine, and (B) hydrogenated cytidine. Both samples are predominantly converted in 5,6-dihydrouridine. The anticipated 5,6-dihydrocytidine is shown as a minor product indicate by the black arrows.

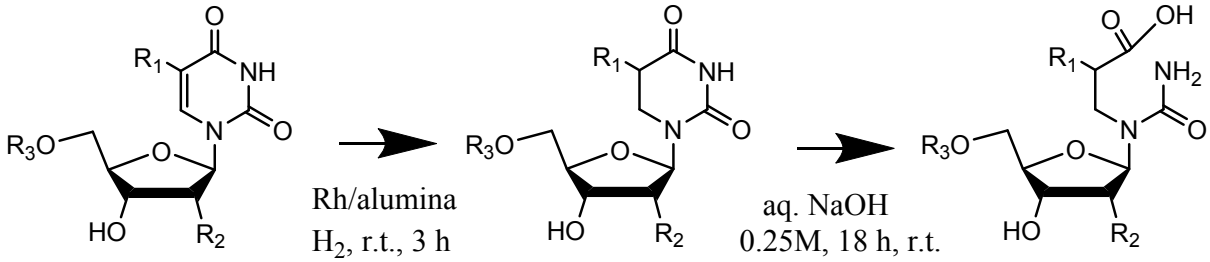

Scheme 1: Catalytic hydrogenation and alkaline-catalyzed ring opening of pyrimidine sugar nucleosides, nucleotide phosphates, and nucleosides. R_1 is H or CH_3, R_2 is H or OH, R_3 is H, phosphate, pyrophosphate, or a monosaccharide-1-pyrophosphate.

Declaration of interests

☒ The authors declare that they have no known competing financial interests or personal relationships that could have appeared to influence the work reported in this paper.

☐The authors declare the following financial interests/personal relationships which may be considered as potential competing interests: